On the origin of the effect of pH in ORR for non-doped and edge-type quaternary N-doped metal-free carbon-based catalysts.

Javier Quílez-Bermejo[a], Karol Strutyński[b], Manuel Melle-Franco[b], Emilia Morallón[c], Diego Cazorla-Amorós*[a]

[a]Departamento de Química Inorgánica and Instituto de Materiales. Universidad de Alicante, Ap. 99, 03080, Alicante, Spain

[b]CICECO – Aveiro Institute of Materials, Department of Chemistry, University of Aveiro, 3810-193 Aveiro, Portugal

[c]Departamento de Química Física and Instituto de Materiales. Universidad de Alicante, Ap. 99, 03080, Alicante, Spain.

*corresponding author: cazorla@ua.es

Keywords

Oxygen reduction reaction, experimental chemistry, computational modelling, carbon-based catalysts, nitrogen doping, pH effect.

Abstract

Metal-free carbon-based catalysts have gained much attention during the last 15 years as an alternative towards the replacement of platinum-based catalysts for the oxygen reduction reaction. However, carbon-based catalysts only show promising catalytic activity in alkaline solution. Concurrently, the most optimized polymer electrolyte membrane fuel cells use protonic exchange membranes. This means that the cathode electrode is surrounded by a protonic environment in which carbon materials show poor performance, with differences above 0.5 V in E_{ONSET} for non-doped carbon materials. Therefore, the search for highly active carbon-based catalysts is only possible if we first understand the origin of the poor electrocatalytic activity of this kind of catalysts in acidic conditions. We address this matter through a combined experimental and modelling study which yields fundamental principles on the origin of the pH effects in ORR for carbon-based materials. This is relevant for the design of pH-independent metal-free carbon-based catalysts.

Introduction

The oxygen reduction reaction is one of the determining limiting factors in polymer electrolyte membrane fuel cells (FC) because of the high overpotential and low reaction rate[1,2]. Platinum is nowadays the most catalytic material towards ORR; however, platinum-based electrodes have important disadvantages, such as high cost, low durability or low resistance towards methanol and CO poisoning[3]. These limitations make highly desirable the replacement of this precious metal by other materials. In this sense, carbon materials have been proved as a promising alternative towards platinum replacement because of their high catalytic activity along with more suitable characteristics[4]. In non-doped carbon materials, the ORR catalytic activity is linearly correlated with the amount of active sites or active surface area as determined from O_2

chemisorption[5]. However, it is also well-known, since the pioneer work published by K. Gong et al[6], that the incorporation of nitrogen heteroatoms generates active sites with much higher activity than the obtained by heteroatom-free carbon materials. This is in agreement with a recent study in which a highly porous carbon was doped with N atoms, but without modifying other parameters such as porosity, showing a significant improvement in activity towards the ORR[7]. Unfortunately, the high catalytic activity of N-doped carbon materials has only been demonstrated in an alkaline electrolyte, whereas in an acidic electrolyte, the performance of metal-free carbon-based catalysts suffers an important decrease in terms of activity[8,9].

This is relevant since heretofore the most developed, and commercially available, polymer electrolyte membranes for the fuel cells are proton exchange membranes[10–12]. This means that the cathode electrode, in these conditions, is surrounded by an acidic environment. Thus, the catalytic activity of those carbon-based materials in the alkaline electrolyte is inefficient for the current polymer electrolyte membrane fuel cells. Therefore, efforts should be applied to the improvement of carbon-based catalysts for their application in an acidic environment. However, there is still a consistent lack of knowledge regarding the performance and reaction mechanism of those catalysts in a protonic electrolyte. The fundamental reasons why carbon materials (doped or not) show poor catalytic activities towards oxygen reduction reaction in acidic environments are still unknown. Nevertheless, some works have tried to explain the reasons of this pH dependence. In a previous work, Noffke et al. addressed the reasons for the pH-dependent behaviour with computational models[13]. These authors suggested the 2 electron pathway as the preferred route in acidic environment and 4 electrons pathway as the preferred route in alkaline solutions, however, most of the experimental works available show the opposite behaviour [8,14–16]. This fact is pointed out in the work of

Behan et al.[17]. They evaluated the performance of different N-doped carbon materials towards ORR as a function of the pH, where a clear decrease of the catalytic activity and higher selectivity towards water production were observed for all carbon-based materials in acidic media. Moreover, the authors suggested that this pH effect was augmented if the ORR takes place in active sites generated by quaternary nitrogen species. Other previous experimental work[18] corroborated this aspect; the performance of carbon-based catalysts in alkaline environment is higher than in acidic media. However, the reasons of this pH dependence are still contradictories and unclear.

In this work, we fill this gap providing a coherent understanding of the effect of pH on the catalytic activity of non-doped and N-doped carbon materials through a combined experimental and computational study. To this end, a non-doped carbon material and a selectively N-doped carbon material have been tested as electrocatalysts in both environments. Computational modelling, based on Density Functional Theory (DFT), has been performed providing a matching interpretation for the different behaviour for non-doped and N-doped carbon materials in ORR catalytic activity in different electrolytes.

Experiments and computational methods

Materials and synthetic procedure.

Polyaniline was obtained from the polymerization of aniline monomers, according to our previous publications[19,20]. N-doped carbon material was obtained as reported in a previous study, through a double-stage heat treatment of polyaniline[20]. This specific double stage heat treatment enables the synthesis of a N-doped carbon material with only one nitrogen species; edge-type graphitic nitrogen functional group[20].

Characterization.

Transmission Electron Microscopy (TEM) was employed to characterize the morphology of the sample. N_2-adsorption isotherm analyses at -196 ºC were used to determine the textural properties of the material. The apparent surface area was obtained from BET theory. Micropore volume was calculated from the Dubinin-Radushkevich equation. Raman spectroscopy was carried out to get information about the structural order of the samples. X-ray photoelectron spectroscopy (XPS) was performed to evaluate the oxidation states of the nitrogen functionalities. The N1s spectra were deconvoluted by employing least-squares fitting with Gaussian-Lorentzian curves. More detailed description of equipments and procedures for the above mentioned physicochemical characterization can be found in our previous works[19,20].

The electrochemical characterization and electrocatalytic properties towards the ORR were evaluated through a rotating ring-disk electrode. The sample was deposited onto a glassy carbon disk electrode through drop-casting method. Further details can be found in our previous work[20].

ORR catalytic activity was studied through linear sweep voltammetry curves (LSV) between 1.0 and 0.0 V vs RHE at different rotation rates in both alkaline and acidic electrolytes: 0.1 M KOH and 0.1 M H_2SO_4 solution, respectively. Moreover, the number of transferred electrons was calculated from the Pt ring electrode, which was held at 1.5 V during ORR measurements, as follows:

$$n = \frac{4I_d}{I_d + I_r/N}$$

Computational Modelling.

Density functional theory (DFT) models at the M06-2X/6-31G(d) level used thorough this work were computed with Gaussian 09[21] with restricted and unrestricted

Hamiltonians for closed-shell (S=0) and open-shell (S=1/2) systems, respectively. The changes in energy for ORR stages were calculated as the difference in free energy from the solvation optimized geometries and are reported in eV (1 Hartree = 27.2116 eV).

The free energy diagrams of ORR have been computed according to Norskov model[22]. The model structures used consist of finite graphene carbon monolayers (or flakes) with 72 and 86 atoms for the non-doped carbon flake and N-doped carbon flake, respectively. The non-doped and N-doped carbon configurations and ORR intermediates were computed as singlets or doublets. A triplet state was used to compute the oxygen molecule. Tables S1, S2 and S3 include the most important numerical values of the free energies for each ORR step.

Results and Discussion

Experimental results

The non-doped carbon material was a commercial carbon black while the N-doped carbon material was prepared from double-stage heat treatment of polyaniline which enables the selective formation of quaternary nitrogen species[20]. The double heat treatment of polyaniline was performed, first, under oxygen-containing atmosphere to favour the development of porosity in the resultant carbon material and, secondly, under inert atmosphere at 1200ºC to tailor the nitrogen functionalities. The resultant N-doped carbon material was characterized in detail by TEM, N_2-adsorption isotherms at -196ºC, Raman spectroscopy and XPS. TEM images (Figure 1a) display the laminar morphology of N-doped carbon material, typical of PANI-derived carbon materials[16]. The N_2-adsorption isotherm (Figure 1b) shows that the material has both a high surface area of 1400 $m^2 \cdot g^{-1}$ and a micropore volume of 0.51 $cm^3 \cdot g^{-1}$. This N_2-adsorption profile is characteristic of carbon materials with highly developed microporosity[23]. Raman spectra (Figure 1c) contains the characteristic D (at around 1350 cm^{-1}) and G (at around

1600 cm^{-1}) bands of sp^2 based carbon materials and the spectrum is typical of carbon materials with low structural ordering.

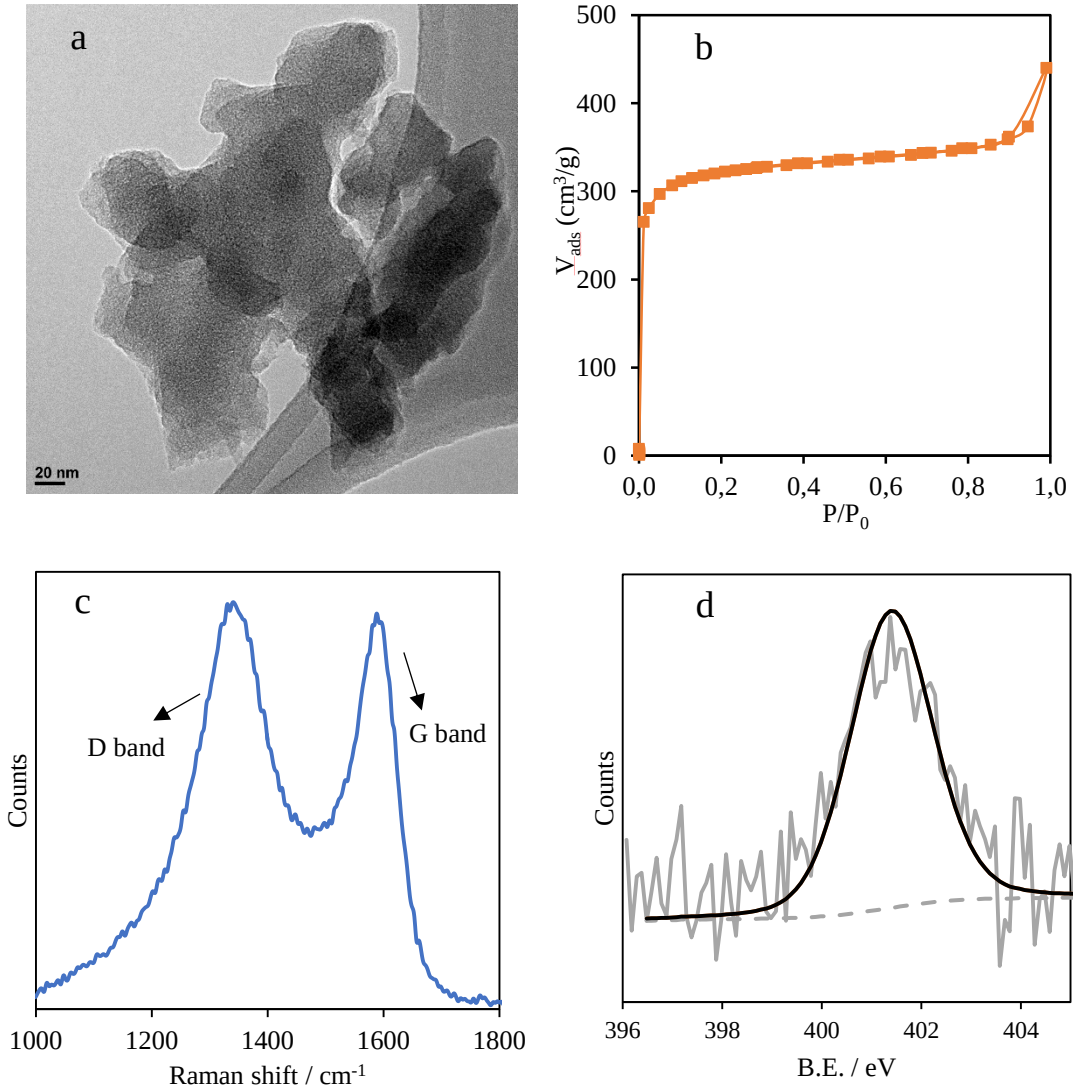

Figure 1: (a) TEM images, **(b)** N2-adsorption isotherm at -196ºC, **(c)** Raman spectra and **(d)** N1s spectra of N-doped carbon material obtained from the double-stage heat treatment of polyaniline.

The nitrogen content was determined by XPS and CHNS analysis. The surface nitrogen content was 1.4 at.%, whereas the CHNS analysis determined that the bulk nitrogen is around 0.7 at.%. This means that there is a heterogeneous distribution of the nitrogen atoms in the material with a higher surface concentration. Furthermore, Figure 1d shows the N1s spectra of the N-doped carbon material, in which solely the presence of quaternary-type nitrogen species is appreciable. These quaternary functionalities are

obtained from a transformation of pyridines and pyridone species into edge-type quaternary nitrogen due to the high temperature used during the second heat treatment[20,24]. More details of the extended characterization and heat treatment of this N-doped carbon material can be found in our previous work[20]. In any case, in the supporting information, we have included the N1s spectra for the sample obtained after the initial treatment in O_2-containing atmosphere up to 1000 ºC, where different N functionalities are observed, and for the final material used in this manuscript (Figure S1). The N1s spectrum for the material used in this work is relevant since edge-type quaternary nitrogen species have been connected to the high catalytic performance of many carbon-based catalysts in alkaline electrolyte[20,24–27]. The obtention of only one nitrogen species in the carbon matrix allows us to evaluate the effect of one nitrogen functional group from experimental and computational modelling points of view.

According to this, non-doped commercial carbon material and the selectively N-doped carbon material, obtained from double heat treatment, were tested as electrocatalysts towards the oxygen reduction reaction. The electrochemical experiments were run in two conditions: a 0.1 M KOH solution and 0.1 M H_2SO_4 solution. Fig. S2-S5 display the LSV curves at rotation rates from 400 to 2025 rpm for both materials in alkaline and acidic electrolyte. As a summary, Figure 2 includes the LSV curves for all materials in acidic and alkaline medium at a rotation rate of 1600 rpm for comparison purposes. Concerning the non-doped carbon material, the catalytic activity of this material shows an onset potential (E_{ONSET}) of 0.80 V vs RHE and high selectivity towards H_2O_2 formation (number of transferred electrons close to 2) in alkaline solution (orange lines). On the other hand, the same material in acidic solution (blue lines) shows a significant decrease in the catalytic activity, with an E_{ONSET} close to 0.3 V vs RHE. Regarding the selectivity in acidic medium, 4 electrons pathway seems to be the

preferred route. Therefore, the non-doped carbon material seems to reduce oxygen more easily in an alkaline solution with high selectivity towards hydrogen peroxide formation. However, water production predominates under acidic conditions although with higher overpotential.

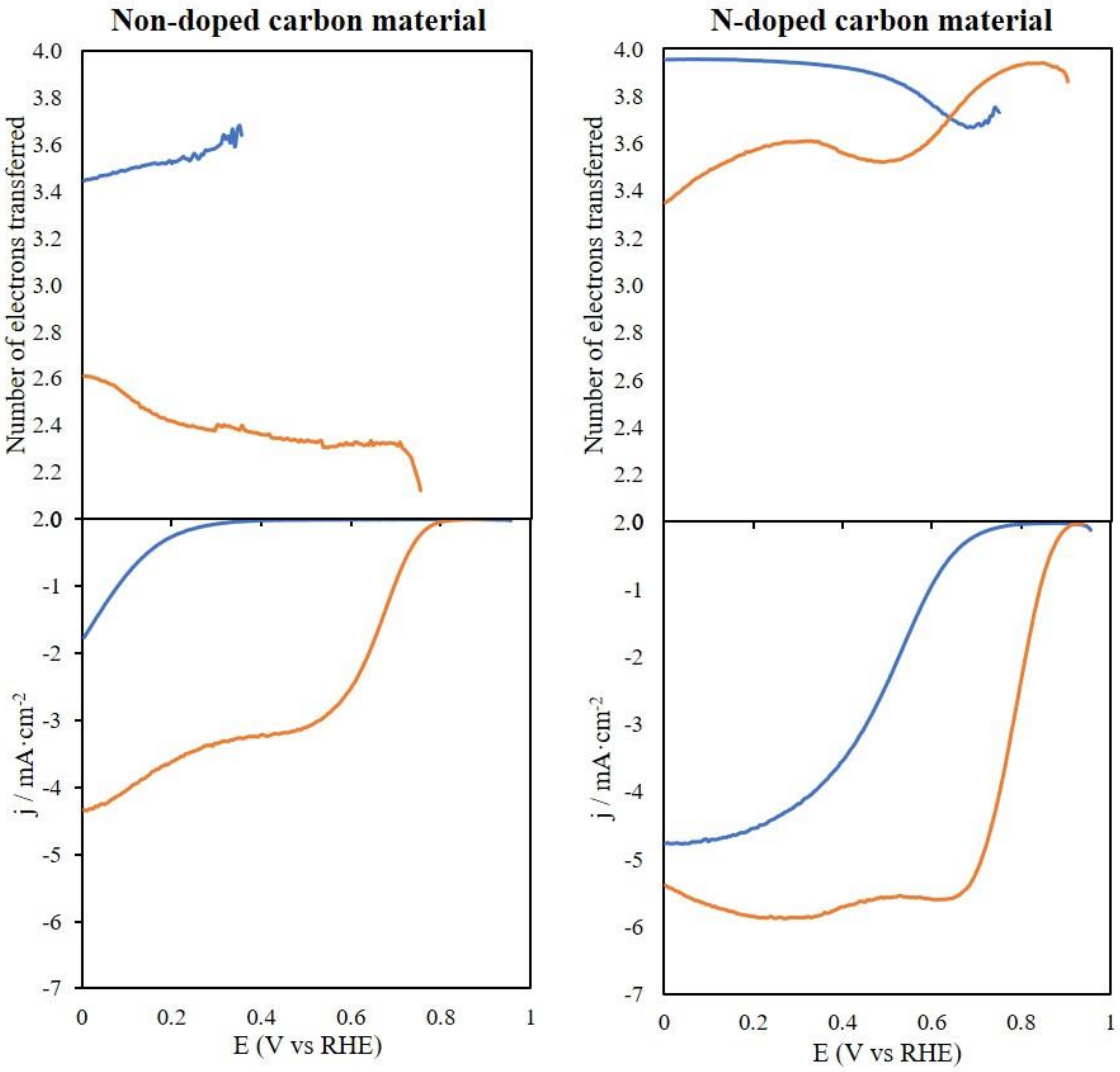

Figure 2: Number of electrons transferred (top) and LSV curves (bottom) for the Non-doped carbon material (left) and the N-doped carbon material (right) in O_2-saturated 0.1 M H_2SO_4 (blue lines) and 0.1 M KOH solutions (orange lines) at 5 mV s^{-1} and 1600 rpm.

Figures 2 also includes the LSV curves of the selectively N-doped carbon material in the same conditions. In alkaline conditions (orange lines), N-doped carbon material shows high catalytic activity with higher E_{ONSET} potential, approaching platinum-like

performance. Moreover, one of the most interesting properties of the N-doped catalyst is its high selectivity towards water formation. However, both limiting current density and onset potential suffer an important decrease in an acidic solution (blue lines). Unfortunately, this decrease is too high (above 0.2 V in E_{ONSET}), making these materials unsuitable to replace commercial platinum catalysts in acidic conditions. Regarding the selectivity, in contrast to the non-doped material, the N-doped carbon material shows a similar number of electrons transferred regardless of the electrolyte used during the electrochemical reaction.

Modelling

In order to get further insights about the different behaviour of non-doped and N-doped carbon materials, computational modelling, based on DFT, was performed (see *Computational modelling* in *Experimental* section for methodology details). A finite non-doped graphene flake was selected to represent the behaviour of non-doped carbon materials as electrocatalysts for ORR. On the other hand, one nitrogen atom was introduced into a similar graphene flake in a zigzag edge-type graphitic position to model the edge-type graphitic nitrogen experimentally obtained in the selective N-doped carbon material (Figure S6). We have only evaluated edge-type graphitic nitrogen in zigzag position (and not armchair), because previous works have shown that only edge-type quaternary nitrogen groups in zigzag position can produce an oxygen reduction through 4 electron pathway[25]. From the experimental results (number of electrons transferred, Figure 2), we assume that the sites at zigzag positions are the main sites in the material. Computations were performed with the M06-2X functional with the 6-31g(d) basis set. All models were embedded in a water continuum with a continuous polarization model as the inclusion of the environment has been found to be fundamental for the quantitative simulation of ORR[28,29]. In addition, this model was

augmented by two water molecules that allow for the explicit formation of hydrogen bonds, following recent studies which demonstrated the necessity of including explicit water molecules to provide improved energetics in models of carbon-based catalysts for ORR[28,30]. The acidic environment and the role of protons in ORR carbon-based catalysts was studied by substituting one water molecule by a hydronium (H_3O^+) cation (Figure S7).

The optimization of the non-doped carbon flake in the presence of one H_3O^+ reveals that the cation binds to the carbon flake, near the negative partial charges in the edges of the carbon material[31], which attract protons due to electrostatic interactions (Figure S8). This indicates that edge sites of a non-doped carbon material are likely surrounded by a protonic environment. Interestingly, this effect is minimized in N-doped carbon flakes. The dopant nitrogen atoms are positively charged and, consequently, repel protons so that a lower local concentration of protons in the vicinity of this nitrogen functionality is expected. In fact, in our static calculations, H_3O^+ molecules moved away from the active sites and prefer to sit on basal positions (Fig. S9). These observations indicate that the acidic pH should have a lower effect in the catalysis of a carbon material doped with this nitrogen functional group because of a lower concentration of protons in the vicinities of the active sites.

Nevertheless, in order to evaluate the influence of H_3O^+ ions in the ORR intermediates, the following sections discuss the free energy diagrams and mechanisms of the ORR in Non-doped and N-doped carbon flakes assuming an equal concentration of protons in the neighbourhoods of the active sites, for comparison purposes.

Non-doped carbon materials

Figure 3 shows the free energies of the most stable configuration for all ORR stages in Non-doped carbon flakes and Figure 4 shows the ORR intermediates in alkaline and acidic media.

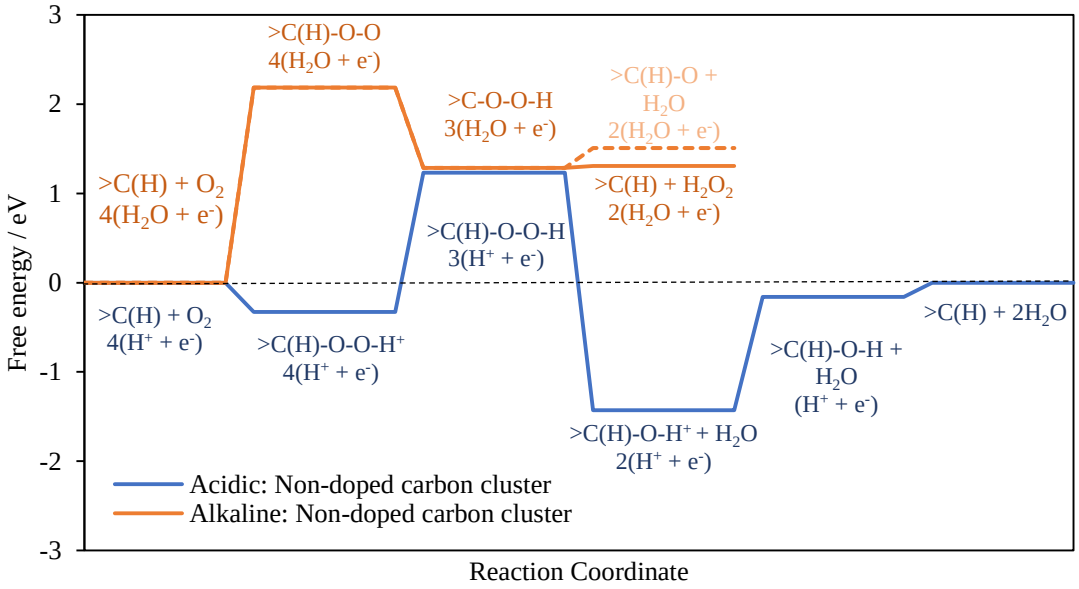

Figure 3: Free energy diagram for the ORR of non-doped carbon flakes in alkaline (orange) and acidic (blue) environments, calculated for 1.23 V NHE.

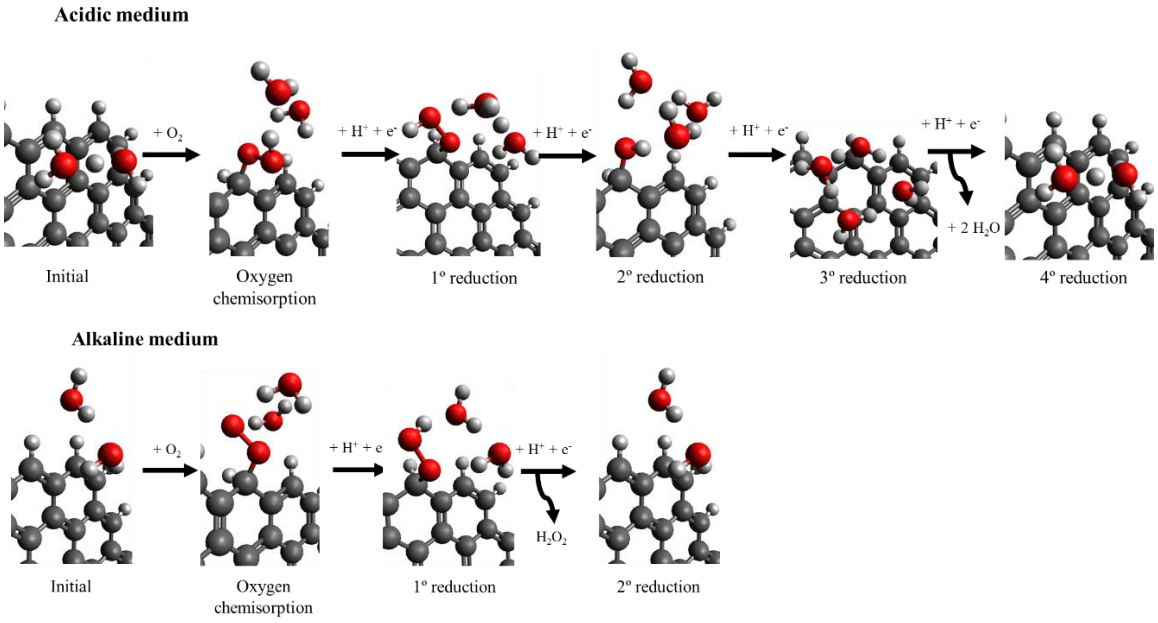

Figure 4: Molecular models for all stages of the ORR of Non-doped carbon flakes in acidic (top) and alkaline (bottom) environments.

Oxygen chemisorption is the first stage of this reaction that can occur through different configurations; terminal or bridging binding modes[32]. In the non-doped carbon flake, oxygen molecules are chemisorbed on terminal positions in both environments. However, the acidic conditions favour strongly the formation of >C(H)-O-O due to the spontaneous protonation of the terminal oxygen atom from the reaction yielding >C(H)-O-O-H^+ (Figure S10). Then, regardless of the electrolyte, the first reduction stage in the non-doped carbon flake leads to an >C(H)-O-O-H intermediate. The key stage is the second reduction step, which may take two forms: the first one leads to the cleavage of the bond between both oxygen atoms (resulting in the formation of one water molecule and a >C(H)-O intermediate) and the second one leads to the cleavage of the carbon and oxygen bond (which results in the formation of hydrogen peroxide). In acidic electrolyte, the most stable configuration is the formation of one water molecule and the >C(H)-O intermediate (Figure 5). This occurs because, in acidic conditions, the >C(H)-O intermediate is strongly stabilized via protonation (>C(H)-O$\cdots H_3O^+$). In contrast, the lack of protons in alkaline environments makes the formation of a >C(H)-O

intermediate energetically less favourable since such stabilization is lower with water molecules. In fact, both mechanisms (formation of >C(H)-O intermediate or hydrogen peroxide) are similar in thermodynamic terms for alkaline environments (see dotted line in Figure 3).

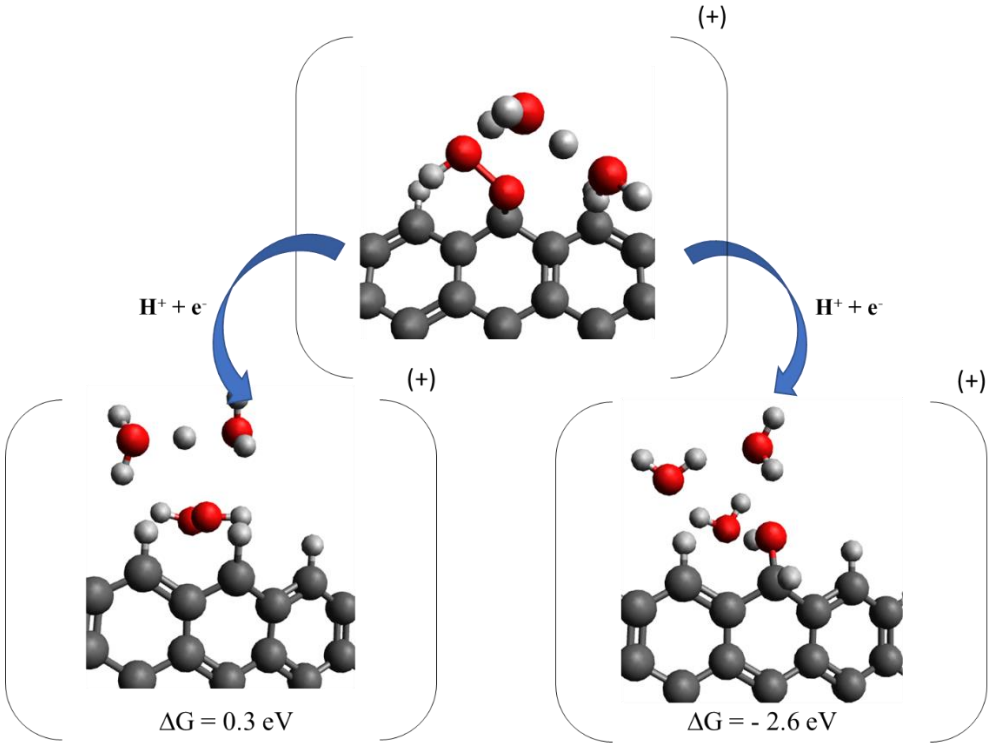

Figure 5: Molecular models and SCF Free energies of the two possible pathways in the second reduction stage by using the carbon flake as electrocatalysts in acidic environment. Carbon in grey, oxygen in red and hydrogen in white.

We computed the Potential Energy Surface (PES) for the desorption of both products (OOH^- and OH^-) in alkaline medium at different distances (Figure 6). Note that the non-doped carbon flake was negatively charged with the aim of accounting for the electron supply. The desorption of OOH^- was found to be energetically more favoured than the desorption of OH^- anions, which indicates that the 2 electron pathway is the preferred pathway for non-doped carbon materials in alkaline medium. This is consistent with the

experimental results. Both desorptions are endothermic, but they do not present additional activation energy barriers.

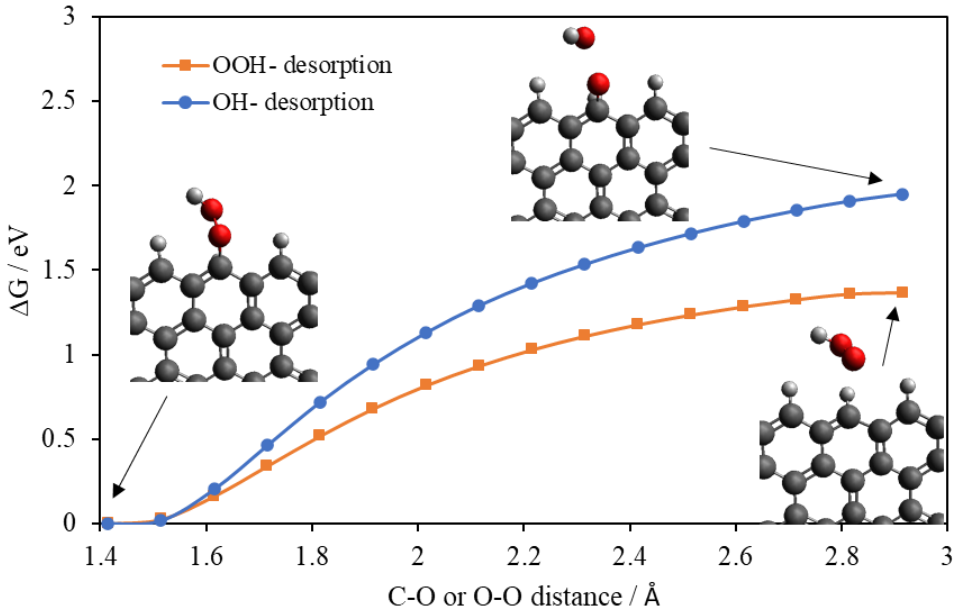

Figure 6: Potential Energy Surface (PES) of the desorption of OOH^- (orange) and OH^- (blue) of the second oxygen reduction stage in which the OOH^- desorption involves the future H_2O_2 formation and OH^- desorption leads to the formation of one water molecule and C-O as a reaction intermediate.

The protonic environment does not only have a direct impact on the selectivity but also plays a fundamental role in the catalytic activity. The protonation of some ORR intermediates under acidic conditions are strongly stabilized so that the required energy to continue with the reaction is considerably higher in a protonic environment than in alkaline conditions (see Figure 3 for free energies). These results are in agreement with the experimental results presented in Figure 2 and can explain the role that different environments play in the catalytic behaviour of Non-doped carbon catalysts.

Nitrogen-doped carbon material

We performed the same computational study on the N-doped carbon flake. Figure 7 shows the free energies of the most stable configuration for all ORR stages in N-doped carbon flakes and Figure 8 shows these ORR intermediates in alkaline and acidic media.

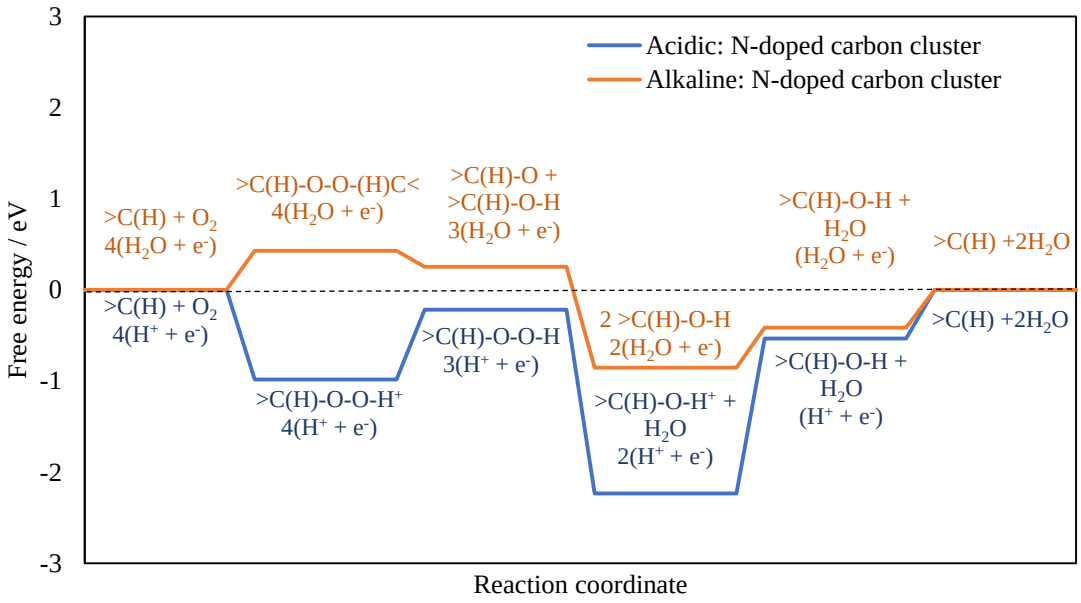

Figure 7: Free energy diagram for the ORR of N-doped carbon flakes in alkaline (orange) and acidic (blue) environments, calculated for 1.23 V NHE.

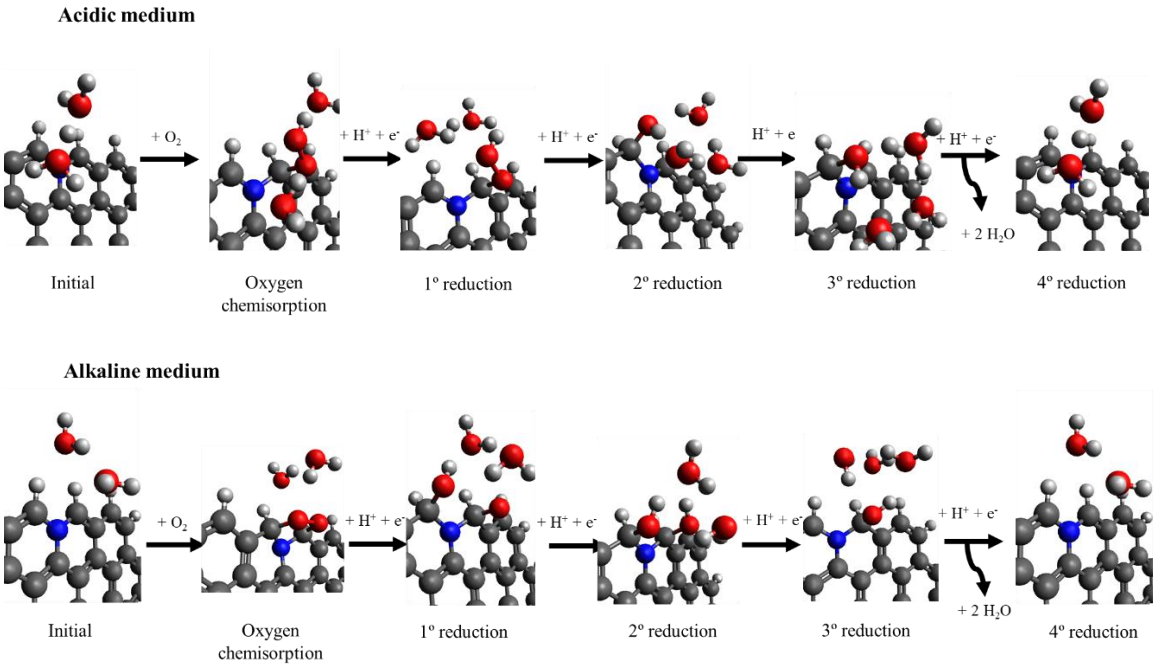

Figure 8: Molecular models for all stages of the ORR of N-doped carbon flakes in acidic (top) and alkaline (bottom) environments.

Unlike Non-doped carbon flakes, the oxygen chemisorption mode is strongly dependent on pH for N-doped carbon flakes. First, in an acidic environment, the terminal binding mode is the only stable configuration in thermodynamic terms. This is again due to the

strong interaction, via protonation, between the terminal oxygen from the >C(H)-O-O and the H_3O^+ ion of the solution, in agreement with what was observed in the non-doped carbon catalysts. The following steps of the reaction are similar to those for the non-doped carbon materials in acidic conditions, where the protonic stabilization of the second ORR intermediate (>C(H)-O-H^+) leads to a 4 electrons pathway and the consequent water formation (see Figure 8 for the mechanisms).

ORR mechanism for edge-type graphitic nitrogen in alkaline conditions has been previously studied in the literature[20,25,26,33–35]. The key part of the mechanism is that the presence of the nitrogen functionality induces chemisorption of the oxygen molecules in a bridging binding mode (>C(H)-O-O-(H)C<) in the absence of protons. This modifies the ORR mechanism compared to the non-doped carbon material in alkaline conditions so that the subsequent reduction stage leads to the cleavage of the O-O bond and, finally, to the formation of two water molecules. The mechanism is included in Figure 8.

Thus, for N-doped carbon flakes, the mechanism is always governed by a 4 electrons pathway regardless of the electrolyte in agreement with the experimental results. In addition, similar to what was observed in the non-doped carbon materials, the differences in activity between electrolytes are related to the high stabilization of the protonated ORR intermediates.

Furthermore, interesting observation can be considered from the obtained results. We find that highly stable C-O-H species are formed in acidic conditions. Hence, through the ongoing reaction, the initial N-C species (with some protons in the vicinity) will be transformed into N-C-O-H, which would constitute a real active phase.

Sabatier´s principle[36] provides the idea that the best catalysts should not bind atoms or molecules too weakly in order to be able to activate them, but neither should bind them too strongly, to allow the reaction to proceed until the desorption of the products. Interestingly, this principle can be extrapolated to the oxygen reduction reaction in these metal-free carbon-based catalysts. In acidic environments, the protonic stabilization in some steps of the ORR induces a too strong binding of the intermediates to the catalytic site, which hampers the completion of the reaction, whereas the lack of protons in alkaline conditions enables an easier termination of the reaction.

Conclusions

In summary, experimental and computational approaches agree on the fact that under the presence of a protonic environment, metal-free carbon-based catalysts suffer an impoverishment in their activity. Computational studies show that this is because of the strong stabilization of some ORR intermediates. Due to such stabilization, the following ORR steps require high energy to occur. Furthermore, the protonic environment does not only modify the catalytic activity of these materials but also changes the mechanism by which ORR takes place. On the one hand, in acidic solution, 4 electrons pathway is the preferred route regardless of whether carbon material is doped with nitrogen or not. On the other hand, in alkaline conditions, ORR for non-doped carbon materials occurs through a 2 electrons pathway, whereas for N-doped carbon materials the preferred reaction mechanism is still the 4 electrons pathway. The understanding of the reasons why metal-free carbon-based catalysts show poorer catalytic activity in a protonic environment should be the guiding principle for the improved design of advanced carbon materials with highly efficient catalysis in acidic conditions. Nevertheless, the negative effect of acidic medium seems to be of great importance for designing advanced N-doped carbon-based catalysts; in terms of E_{ONSET}, 0.2 V for N-doped

carbon materials and 0.5 V for non-doped carbon materials. We hypothesize that for further improvement of carbon-based catalysts, additional functional groups may be needed that may modify the local acid/base properties. However, we believe that the increase in the catalytic properties up to platinum-like performance will be difficult and will remain as a challenge. Probably, the synthesis of adequate alkaline exchange membranes could be one of the options for the technological application of N doped carbon materials catalysts in fuel cells.

Associated content

The Supporting Information is available free of charge on the ACS Publications website.

N1s spectra of PANI-derived carbon obtained from the first heat treatment of polyaniline in oxygen-containing atmosphere at 1000ºC and N1s spectra of the resultant N-doped carbon material utilized in this work, obtained from the double-stage heat treatment of polyaniline. LSV curves of non-doped and N-doped carbon material obtained from double stage heat treatment of polyaniline in 0.1 M H_2SO_4 and 0.1 M KOH solutions. Model structures of non-doped and N-doped carbon flakes. Illustration and net charges of the non-doped and N-doped carbon materials in alkaline and acidic conditions. Free energy differences and rendering of the H_3O^+ position in the non-doped and N-doped carbon flakes. Optimized geometry of the H_3O^+ ion at a non-contact distance of the nitrogen heteroatom as a result of the repulsion charges. Illustration and free energies of the oxygen chemisorption stage by using non-doped carbon flakes in alkaline and acidic environment. Tables of free energies of all ORR intermediates and reagents.

Conflict of interest

The authors declare no conflict of interests.

Acknowledgements

The authors thank Ministerio de Ciencia, Innovación y Universidades and FEDER for financial support (Project RTI2018-095291-B-I00 and ENE2017-90932-REDT) and the Portuguese Foundation for Science and Technology (FCT), under the projects IF/00894/2015 and CICECO-Aveiro Institute of Materials, UIDB/50011/2020 & UIDP/50011/2020, financed by national funds through the FCT/MCTES.

References

(1) Nie, Y.; Li, L.; Wei, Z. Recent Advancements in Pt and Pt-Free Catalysts for Oxygen Reduction Reaction. *Chem. Soc. Rev.* **2015**, *44* (8), 2168–2201.

(2) Stephens, I. E. L.; Bondarenko, A. S.; Grønbjerg, U.; Rossmeisl, J.; Chorkendorff, I. Understanding the Electrocatalysis of Oxygen Reduction on Platinum and Its Alloys. *Energy Environ. Sci.* **2012**, *5* (5), 6744–6762.

(3) Jiao, Y.; Zheng, Y.; Jaroniec, M.; Qiao, S. Z. Design of Electrocatalysts for Oxygen- and Hydrogen-Involving Energy Conversion Reactions. *Chem. Soc. Rev.* **2015**, *44* (8), 2060–2086.

(4) Dai, L.; Xue, Y.; Qu, L.; Choi, H.-J.; Baek, J.-B. Metal-Free Catalysts for Oxygen Reduction Reaction. *Chem. Rev.* **2015**, *115* (11), 4823–4892.

(5) Gabe, A.; Ruiz-Rosas, R.; González-Gaitán, C.; Morallón, E.; Cazorla-Amorós, D. Modeling of Oxygen Reduction Reaction in Porous Carbon Materials in Alkaline Medium. Effect of Microporosity. *J. Power Sources* **2019**, *412*, 451–464.

(6) Gong, K.; Du, F.; Xia, Z.; Durstock, M.; Dai, L. Nitrogen-Doped Carbon

Nanotube Arrays with High Electrocatalytic Activity for Oxygen Reduction. *Science* **2009**, *323* (5915), 760–764.

(7) Mostazo-López, M. J.; Salinas-Torres, D.; Ruiz-Rosas, R.; Morallón, E.; Cazorla-Amorós, D. Nitrogen-Doped Superporous Activated Carbons as Electrocatalysts for the Oxygen Reduction Reaction. *Materials* **2019**, *12* (8), 1346.

(8) Klingele, M.; Van Pham, C.; Fischer, A.; Thiele, S. A Review on Metal-Free Doped Carbon Materials Used as Oxygen Reduction Catalysts in Solid Electrolyte Proton Exchange Fuel Cells. *Fuel Cells* **2016**, *16* (5), 522–529.

(9) Quílez-Bermejo, J.; Morallón, E.; Cazorla-Amorós, D. Metal-Free Heteroatom-Doped Carbon-Based Catalysts for ORR. A Critical Assessment about the Role of Heteroatoms. *Carbon* **2020**, *165*, 434–454.

(10) Ramaswamy, N.; Mukerjee, S. Alkaline Anion-Exchange Membrane Fuel Cells: Challenges in Electrocatalysis and Interfacial Charge Transfer. *Chem. Rev.* **2019**, *119* (23), 11945–11979.

(11) Pan, Z. F.; An, L.; Zhao, T. S.; Tang, Z. K. Advances and Challenges in Alkaline Anion Exchange Membrane Fuel Cells. *Prog. Energy Combust. Sci.* **2018**, *66*, 141–175.

(12) Sun, Z.; Lin, B.; Yan, F. Anion-Exchange Membranes for Alkaline Fuel-Cell Applications: The Effects of Cations. *ChemSusChem* **2018**, *11* (1), 58–70.

(13) Noffke, B. W.; Li, Q.; Raghavachari, K.; Li, L. A Model for the PH-Dependent Selectivity of the Oxygen Reduction Reaction Electrocatalyzed by N-Doped Graphitic Carbon. *J. Am. Chem. Soc.* **2016**, *138* (42), 13923–13929.

(14) Zhang, X.; Yu, D.; Zhang, Y.; Guo, W.; Ma, X.; He, X. Nitrogen- and Sulfur-Doped Carbon Nanoplatelets via Thermal Annealing of Alkaline Lignin with Urea as Efficient Electrocatalysts for Oxygen Reduction Reaction. *RSC Adv.* **2016**, *6* (106), 104183–104192.

(15) Nong, J.; Zhu, M.; He, K.; Zhu, A.; Xie, P.; Rong, M.; Zhang, M. N/S Co-Doped 3D Carbon Framework Prepared by a Facile Morphology-Controlled Solid-State Pyrolysis Method for Oxygen Reduction Reaction in Both Acidic and Alkaline Media. *J. Energy Chem.* **2019**, *34*, 220–226.

(16) Quílez-Bermejo, J.; González-Gaitán, C.; Morallón, E.; Cazorla-Amorós, D. Effect of Carbonization Conditions of Polyaniline on Its Catalytic Activity towards ORR. Some Insights about the Nature of the Active Sites. *Carbon* **2017**, *119*, 62–71.

(17) Behan, J. A.; Iannaci, A.; Domínguez, C.; Stamatin, S. N.; Hoque, K.; Vasconcelos, J. M.; Perova, T. S.; Colavita, P. E. Electrocatalysis of N-Doped Carbons in the Oxygen Reduction Reaction as a Function of PH : N-Sites and Scaffold Effects. *Carbon* **2019**, *148*, 224–230.

(18) Wan, K.; Yu, Z.-P.; Li, X.-H.; Liu, M.-Y.; Yang, G.; Piao, J. H.; Liang, Z. X. PH Effect on Electrochemistry of Nitrogen-Doped Carbon Catalysts for Oxygen Reduction Reaction. *ACS Catal.* **2015**, *5* (7), 4325–4332.

(19) Quílez-Bermejo, J.; Ghisolfi, A.; Grau-Marín, D.; San-Fabián, E.; Morallón, E.; Cazorla-Amorós, D. Post-Synthetic Efficient Functionalization of Polyaniline with Phosphorus-Containing Groups. Effect of Phosphorus on Electrochemical Properties. *Eur. Polym. J.* **2019**, *119*, 272–280.

(20) Quílez-Bermejo, J.; Melle-Franco, M.; San-Fabián, E.; Morallón, E.; Cazorla-

Amorós, D. Towards Understanding the Active Sites for the ORR in N-Doped Carbon Materials through Fine-Tuning of Nitrogen Functionalities: An Experimental and Computational Approach. *J. Mater. Chem. A* **2019**, *7*, 24239–24250.

(21) Gaussian 09, Revision A.02, M. J. Frisch, G. W. Trucks, H. B. Schlegel, G. E. Scuseria, M. A. Robb, J. R. Cheeseman, G. Scalmani, V. Barone, G. A. Petersson, H. Nakatsuji, X. Li, M. Caricato, A. Marenich, J. Bloino, B. G. Janesko, R. Gomperts, B. Mennucci, H. P. Hratchian, J. V. Ortiz, A. F. Izmaylov, J. L. Sonnenberg, D. Williams-Young, F. Ding, F. Lipparini, F. Egidi, J. Goings, B. Peng, A. Petrone, T. Henderson, D. Ranasinghe, V. G. Zakrzewski, J. Gao, N. Rega, G. Zheng, W. Liang, M. Hada, M. Ehara, K. Toyota, R. Fukuda, J. Hasegawa, M. Ishida, T. Nakajima, Y. Honda, O. Kitao, H. Nakai, T. Vreven, K. Throssell, J. A. Montgomery, Jr., J. E. Peralta, F. Ogliaro, M. Bearpark, J. J. Heyd, E. Brothers, K. N. Kudin, V. N. Staroverov, T. Keith, R. Kobayashi, J. Normand, K. Raghavachari, A. Rendell, J. C. Burant, S. S. Iyengar, J. Tomasi, M. Cossi, J. M. Millam, M. Klene, C. Adamo, R. Cammi, J. W. Ochterski, R. L. Martin, K. Morokuma, O. Farkas, J. B. Foresman, and D. J. Fox, Gaussian, Inc., Wallingford CT, 2016.

(22) Nørskov, J. K.; Rossmeisl, J.; Logadottir, A.; Lindqvist, L.; Kitchin, J. R.; Bligaard, T.; Jónsson, H. Origin of the Overpotential for Oxygen Reduction at a Fuel-Cell Cathode. *J. Phys. Chem. B* **2004**, *108* (46), 17886–17892.

(23) Thommes, M.; Kaneko, K.; Neimark, A. V; Olivier, J. P.; Rodriguez-reinoso, F.; Rouquerol, J.; Sing, K. S. W. Physisorption of Gases , with Special Reference to the Evaluation of Surface Area and Pore Size Distribution (IUPAC Technical Report). *Pure and Applied Chemistry* **2015,** 87, 1051-1069.

(24) Sharifi, T.; Hu, G.; Jia, X.; Wågberg, T. Formation of Active Sites for Oxygen Reduction Reactions by Transformation of Nitrogen Functionalities in Nitrogen-Doped Carbon Nanotubes. *ACS Nano* **2012**, *6* (10), 8904–8912.

(25) Quílez-Bermejo, J.; Morallón, E.; Cazorla-Amorós, D. Oxygen-Reduction Catalysis of N-Doped Carbons Prepared: Via Heat Treatment of Polyaniline at over 1100 °C. *Chem. Commun.* **2018**, *54* (35), 4441–4444.

(26) Ikeda, T.; Boero, M.; Huang, S. F.; Terakura, K.; Oshima, M.; Ozaki, J. Carbon Alloy Catalysts: Active Sites for Oxygen Reduction Reaction. *J. Phys. Chem. C* **2008**, *112* (38), 14706–14709.

(27) Quílez-Bermejo, J.; Morallón, E.; Cazorla-Amorós, D. Polyaniline-Derived N-Doped Ordered Mesoporous Carbon Thin Films: Efficient Catalysts towards Oxygen Reduction Reaction. *Polymers* **2020**, *12* (10), 2382.

(28) Reda, M.; Hansen, H. A.; Vegge, T. DFT Study of Stabilization Effects on N-Doped Graphene for ORR Catalysis. *Catal. Today* **2018**, *312*, 118–125.

(29) Lile, J. R. D.; Zhou, S. Theoretical Modeling of the PEMFC Catalyst Layer: A Review of Atomistic Methods. *Electrochim. Acta* **2015**, *177*, 4–20.

(30) Yu, L.; Pan, X.; Cao, X.; Hu, P.; Bao, X. Oxygen Reduction Reaction Mechanism on Nitrogen-Doped Graphene: A Density Functional Theory Study. *J. Catal.* **2011**, *282* (1), 183–190.

(31) Louis, E.; San-Fabián, E.; Chiappe, G.; Verges, J. A. Electron Enrichment of Zigzag Edges of Armchair-Oriented Graphene Nano-Ribbons Increases Their Stability and Induces Pinning of Fermi Level. *Carbon* **2019**, *154*, 211–218.

(32) Wu, K. H.; Wang, D. W.; Su, D. S.; Gentle, I. R. A Discussion on the Activity

Origin in Metal-Free Nitrogen-Doped Carbons for Oxygen Reduction Reaction and Their Mechanisms. *ChemSusChem* **2015**, *8* (17), 2772–2788.

(33) Hou, X.; Hu, Q.; Zhang, P.; Mi, J. Oxygen Reduction Reaction on Nitrogen-Doped Graphene Nanoribbons: A Density Functional Theory Study. *Chem. Phys. Lett.* **2016**, *663*, 123–127.

(34) Bao, X.; Nie, X.; Von Deak, D.; Biddinger, E. J.; Luo, W.; Asthagiri, A.; Ozkan, U. S.; Hadad, C. M. A First-Principles Study of the Role of Quaternary-N Doping on the Oxygen Reduction Reaction Activity and Selectivity of Graphene Edge Sites. *Top. Catal.* **2013**, *56* (18–20), 1623–1633.

(35) Chai, G. L.; Hou, Z.; Shu, D. J.; Ikeda, T.; Terakura, K. Active Sites and Mechanisms for Oxygen Reduction Reaction on Nitrogen-Doped Carbon Alloy Catalysts: Stone-Wales Defect and Curvature Effect. *J. Am. Chem. Soc.* **2014**, *136* (39), 13629–13640.

(36) Che, M. Nobel Prize in Chemistry 1912 to Sabatier: Organic Chemistry or Catalysis? *Catal. Today* **2013**, *218–219*, 162–171.

Table Of Contents graphic

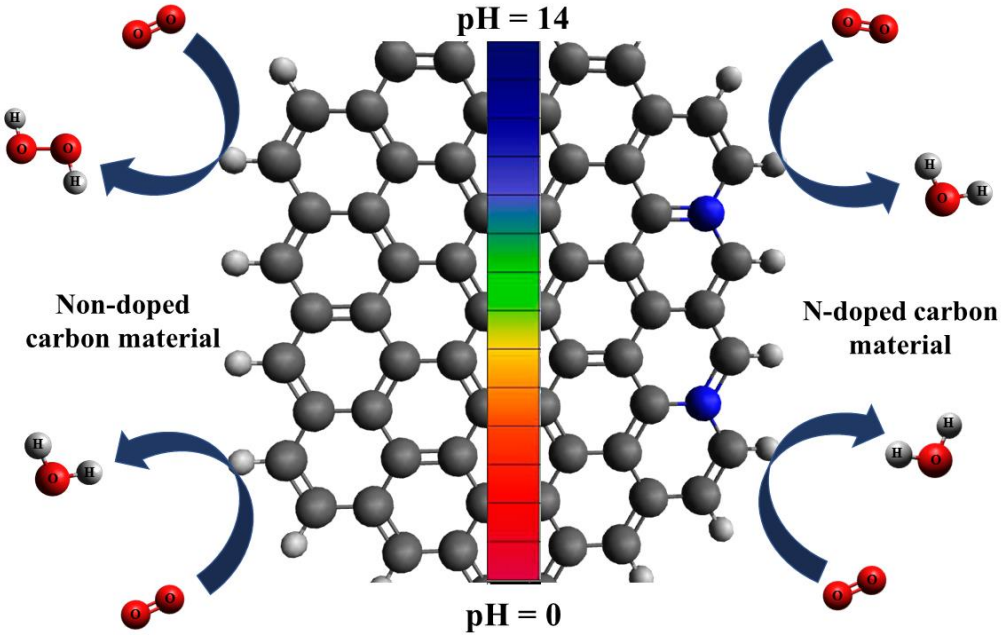
pH = 14
Non-doped
carbon material
N-doped carbon
material
pH = 0